Marine Geology 275 (2010) 96–109

Contents lists available at ScienceDirect

Marine Geology

journal homepage: www.elsevier.com/locate/margeo

Short-term morphological responses and developments of Banda Aceh coast, Sumatra Island, Indonesia after the tsunami on 26 December 2004

E. Meilianda [a,b,*], C.M. Dohmen-Janssen [b], B.H.P. Maathuis [c], S.J.M.H. Hulscher [b], J.P.M. Mulder [b]

[a] Civil Engineering Department, Engineering Faculty, Syiah Kuala University, Jalan Tgk. Abdul Rauf No. 7 Darussalam, Banda Aceh 23111, Indonesia
[b] Water Engineering and Management (WEM), University of Twente, PO Box 217, 7500 AE Enschede, The Netherlands
[c] Water Resources Department, Faculty of Geo-information Science and Earth Observation (ITC), University of Twente, PO Box 6, 7500 AA Enschede, The Netherlands

ARTICLE INFO

Article history:
Received 7 July 2008
Received in revised form 29 April 2010
Accepted 30 April 2010
Available online 7 May 2010

Communicated by D.J.W. Piper

Keywords:
tsunami
land subsidence
coastal morphological development
shoreline
Digital Elevation Model
spatial analysis

ABSTRACT

The destructive earthquake and tsunami waves have caused sudden and immense changes in the morphology of the low-lying coast of Banda Aceh, Sumatra Island, Indonesia on 26 December 2004. Data from different sources and different instants in time used in this study to investigate the morphological responses and developments of two coasts that were affected by the tsunami near Banda Aceh; i.e. Ulee Lheue on the northwest coast and Lampu Uk on the west coast. The objective was to quantify the morphological changes of the two coasts that were affected by the tsunami and tectonic land subsidence, and their subsequent short-term developments. Interestingly, the foreshore zone of the two coasts after six months showed a contrasting development relative to their pre-tsunami's morphological state. Ulee Lheue, on the northwest coast, experienced ongoing erosion of about 15% of the total sediment loss due to the tsunami and land subsidence. The erosion effect from the land subsidence is not pre-dominant in this coast, compared to the erosion that was caused by the tsunami waves. Keeping in mind that the coast is a sand-poor environment, the coastal process under normal condition could not keep pace with not only the sudden loss of sediment due to land subsidence, but also to a greater extent, due to lack of sediment availability in the coastal system to replace the amount of sediment loss due to the tsunami waves. On the other hand, the amount of sediment regain in Lampu Uk was 60% out of the total sediment loss due to the tsunami and land subsidence. It compensated to a great extent the sudden loss of sediments due to land subsidence which was greater than the one on the northwest coast. The wide and shallow inner shelf and higher wave energy in this coastal region can be the controlling factor of this temporary sediment storage and the rapid accretion.

1. Introduction

Recently, the world experienced a huge natural disaster in the form of the earthquake and tsunami in the Indian Ocean on 26 December 2004. A fault displacement between the Indian oceanic and Eurasian continental plates to the west of Sumatra Island caused a submarine earthquake with a magnitude of $M = 9.0$ on the Richter scale (Stein and Okal, 2005; Waltham, 2005). In the following 20 min, it triggered huge tsunami waves propagating across the Indian Ocean, destroyed the bordering coastal areas and caused a massive loss of human life in countries bordering the Indian Ocean.

The low-lying city of Banda Aceh on the northern tip of Sumatra was one of the worst affected regions and experienced massive casualties and destruction of property, as it was close (ca. 150 km) to the source of the earthquake. The loss of human life recorded was the highest at about two-thirds of the total of 300,000 casualties.

The destructive tsunami waves caused sudden and immense changes in the morphology of the low-lying coast of Banda Aceh. Significant amounts of coastal sediment were scoured, transported and deposited back and forth along the path of tsunami waves, causing immense sediment re-distributions over the entire coast (Jaffe et al., 2006; Narayana et al., 2007; Umitsu et al., 2007; Paris et al., 2007). Tectonic subsidence is suspected to have occurred (Gibbons and Gelfenbaum, 2005; Jaffe et al., 2006; Meltzner et al., 2006; Subarya et al., 2006) as a consequence of the earthquake on 26 December 2004 as well as the one on 28 March 2005 (with a magnitude of $M = 8.0$ on the Richter scale).

Studies into the impact of a tsunami on coastal areas have been of interest to scientists for many years. These studies mostly address the analysis of sub-aerial sediment distributions by the tsunami waves (e.g. Narayana et al., 2007; Paris et al., 2007 at the west coast of Banda

* Corresponding author. Present address: MARUM – University of Bremen, Leobenerstrasse D-28359 Bremen, Germany. Tel.: +49 421 218 65864; fax: +49 421 218 65515.
E-mail addresses: emeilianda@gmail.com (E. Meilianda), c.m.dohmen-janssen@utwente.nl (C.M. Dohmen-Janssen), maathuis@itc.nl (B.H.P. Maathuis), s.j.m.h.hulscher@utwente.nl (S.J.M.H. Hulscher), j.p.m.mulder@utwente.nl (J.P.M. Mulder).

0025-3227/$ – see front matter © 2010 Elsevier B.V. All rights reserved.
doi:10.1016/j.margeo.2010.04.012

Aceh). Gelfenbaum and Jaffe (2003) used their analysis of the subaerial sediment deposits and distribution to reconstruct the tsunami wave flow pattern in Papua, Indonesia, while Umitsu et al. (2007) used them to examine how landforms affect the tsunami flow on the west coast of Banda Aceh. Noda et al. (2007) improved the understanding of the change in offshore sediment characteristics after the tsunami caused by the Tokachi-oki earthquake in Japan in 2003, by using a combined approach of sediment sampling and modelling. At present, estimates of the real-time sediment transport processes during the tsunami of 2004 remain speculative (Paris et al., 2007). Despite these growing interests, there is little discussion on the morphological adjustment and its subsequent development after the tsunami and the combining effect of a land subsidence due to the earthquake. This is mainly due to the lack of available data, such as bathymetry, sediment characteristics or wave climate, especially during the tsunami itself. In addition, pre- and post-event data were poorly archived, resulting in a gap of knowledge on the morphological development of the affected coasts.

Sudden and extreme coastal hazard may give significant impact to a coastal area. Morton et al. (1994) identified four stages of short-term recovery process of the sand-rich Galveston coast on the southeastern Texas, USA after was hit by Alicia, a category-3 hurricane. Nevertheless, the impact may also be irreversible (e.g. due to sudden land subsidence or uplift). For instance, Sallenger et al. (2007) revealed a high degree of shoreline variability (chaotic shoreline) and severely breached barrier islands on the Dauphin Island, Alabama, USA as the immediate impact of the Hurricane Katrina of 2005.

We put forward that the ability of a coast to recover in a short-term after the large scale earthquake and tsunami depends on the extent of the given impact by these extreme events. The extent of the impact depends on the geomorphic settings inherited to the coast. The subsequent morphological development is determined by the extent of the impact itself, the geomorphic settings in which the sediment redistributed and the available sediment that are movable by the normal wave condition after the tsunami event.

In order to attest the above-mentioned hypothesis, this study is aimed to quantify the morphological changes of two coasts near Banda Aceh that were affected by the 2004 tsunami and tectonic land subsidence, and their subsequent short-term developments. The main research question put forward is on how coasts with different geomorphic settings respond to and develop after such huge earthquake and tsunami events.

In this study, data such as an aerial photo mosaic, satellite images, bathymetry and coastal topography at certain points in time before and after the tsunami (i.e. from 2001 to 2007) were used to analyse the-direct-impact of the tsunami and the short-term morphological development of the coasts about two years after the tsunami. All data involved in this study were processed through GIS-based procedures such as geo-referencing, shoreline digitizing, and Digital Elevation Model (DEM) generation. In addition, two field visits were conducted in June 2005 and August 2006. Data analysis and interpretation were validated using observations from the two field visits and additional information from the literature.

2. Study locations and data overview

2.1. Study locations

Banda Aceh is located in the triangular coastal plain at the northwest tip of Sumatra Island, Indonesia. The coastal plain is surrounded by the Indian Ocean on the west coast, the Andaman Sea which is enclosed by small islands in the north, and the Malacca Straits in the northeast (inset of Fig. 1a). Two study locations were selected (Fig. 1b and c): i) Ulee Lheue (pronounced *Oolé leu*) on the northwest coast, and ii) Lampu Uk (pronounced *Lampoo Ook*) on the west coast of Banda Aceh. They were selected because the resolution of the available data (either spatially or temporally) is highest in these areas. The lengths of the Ulee Lheue and Lampu Uk sections are about 1 km and 3 km, respectively.

2.1.1. Ulee Lheue, northwest coast

The coast of Ulee Lheue has a flat alluvial hinterland which is separated by a small shore-parallel lagoon facing a narrow and convex-shape shoreface developed by the alluvial progradation during the late Holocene (Meilianda, 2009). The average elevation of the barrier was about +1.5 m above Mean Low Water Level (MLWL). The foreshore slope in front of the seawall was between 1:10 and 1:25, adjacent on the seaward with ca. 2.5 km wide of shoreface which slope was 1:100 and abruptly steepened from here on to the inner shelf of −250 m depth (Fig. 1a). The beach consists of loose fine quartz sand of D_{50} = 120–140 μm (UP-PSDA, 2003).

We derived the wave climate of the Banda Aceh coast from eleven-year daily wind data records from 1995 to 2005. The wind data were recorded by the Department of Meteorology and Geophysics in Banda Aceh, and subsequently translated into statistical wave heights and periods as functions of wind velocity, duration and fetch (CERC, 1992).

About 53% of the waves approach the coast with a significant wave height of 1.0 m with a period of 3 s, which was influenced by the southwest monsoon between April and September. During the northeast monsoon between October and March, 30% of the waves were approaching from the northeast with a significant wave height of also 1.0 m and a period of 4.5 s. These numbers show that the northwest coast of Banda Aceh is typically a low energy coast.

In considering the geomorphic settings of the Banda Aceh coast, Meilianda (2009) suggested that waves coming from the northwest may induce a certain amount of cliff erosion, i.e. from the Ujong Pancu headland (Fig. 1a). However, only a small amount would feed the Ulee Lheue coast, otherwise, the eroded cliff material may be deposited into the submarine valley associated with the Sumatran Fault System (SFS) further offshore. We understood that seasonal change was not important in this particular coastal section (personal communication with Dr. Wong Poh Poh of the National University of Singapore). Moreover, the Ulee Lheue coast is not a recipient of sediment supplied from the Krueng Aceh River. This suggests that Ulee Lheue is a sand-poor coastal environment.

Before the tsunami, a one-km seawall was present along Ulee Lheue beach at the northeast side of Krueng Cangkoy river mouth (Fig. 1b). A short stretch of the beach between the seawall and the ferry port was unprotected by any structures. Due to the tsunami in 2004, about half-a-km unprotected beach ridge section was breached, separating the Ulee Lheue village from the Ferry port and causing inundation further landward, especially during the high tides. As an immediate protective response, the local authority planned to set up a new seawall for the entire 25-km-long northwest coastal stretch of Banda Aceh. The construction started in 2005 and was half-completed (i.e. from Ulee Lheue to the west part of the Alue Naga Floodway channel) in January 2007.

2.1.2. Lampu Uk, west coast

Hydrometric data of the west coast was extremely lacking. From a local coastal safety project report (Anonymous, 1997) we obtained the significant wave height and period as to be 2.5 m and 5 s, respectively without further explanation on the type of data and analysis. The prevailing waves are coming from the southwest and presumably corresponding to persistent south–north longshore sediment transport. Thus, the west coast has higher wave energy than the northwest coast. The west coast consists of sandy beach with D_{50} = 140–250 μm of grain size. The coastal plain was generally situated higher than +2.5 m above MHWL.

Lampu Uk beach is located between a small headland in the north and the Krueng Reba river mouth in the south (Fig. 1c). An offshore coral reef system existed in the middle of this 3.3-km coastal stretch. A

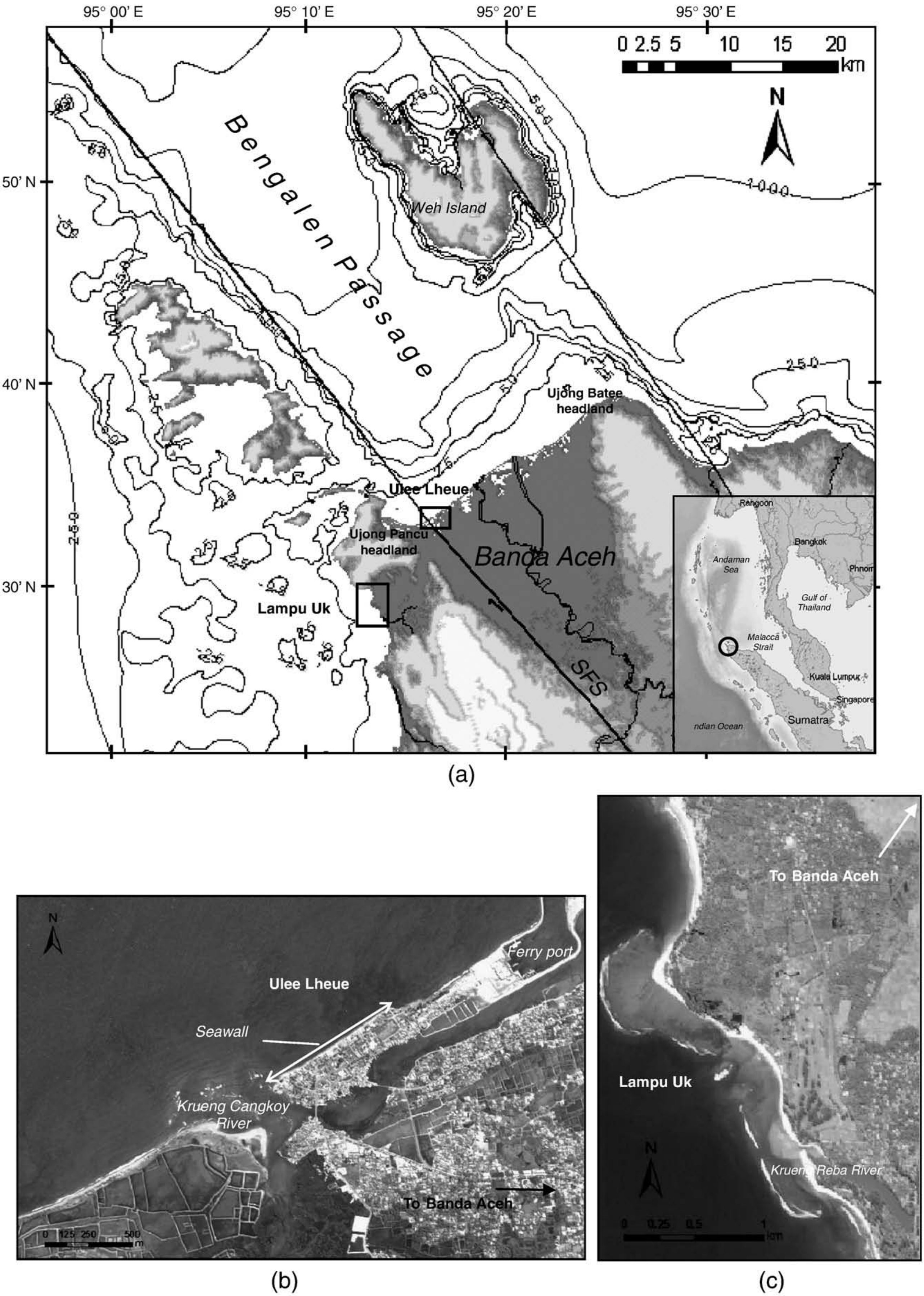
95° 00' E
95° 10' E
95° 20' E
95° 30' E
05° 50' N
05° 40' N
05° 30' N
0 2.5 5 10 15 20 km
N
Bengalen Passage
Weh Island
-1000
-250
Ujong Batee headland
Ulee Lheue
Ujong Pancu headland
Banda Aceh
Lampu Uk
SFS
Rangoon
Bangkok
Andaman Sea
Gulf of Thailand
Malacca Strait
Kuala Lumpur
Singapore
Sumatra
ndian Ocean
(a)
N
Ferry port
Ulee Lheue
Seawall
Krueng Cangkoy River
To Banda Aceh
0 125 250 500 m
(b)
To Banda Aceh
Lampu Uk
N
Krueng Reba River
0 0.25 0.5 1 km
(c)

Table 1
Available data sources and their acquisitions.

Image data		Date	Local time (hr/mn/sc)	Tidal elevation[a] (m)	Spatial resolution (m)
Bathymetry[b]		April 2001	N/A	N/A	0.5 (vertical)
Satellite image[c]	West (Quickbird)	13 Jan 2002	11:12:39	0.7 (MLWL)	2.5
	Northwest (IKONOS)	23 Jun 2004	10:54:29	0.5 (MLWL)	2.5
	West and northwest (IKONOS)	30 Dec 2004	10:55:41	1.2 (1 h. before MHWL)	2.5
Ortho-rectified aerial photo mosaic[d]		06 Jun 2005	Ca. 08:30:00	1.5 (MHWL)	0.3 (basemap)
Coastal topography map[e]		06 Jun 2005	Ca. 08:30:00	1.5 (MHWL)	0.5 (vertical)
Bathymetry 2[f]		Jan 2006	N/A	N/A	0.5 (vertical)
Bathymetry 3[f]		Jan 2007	N/A	N/A	0.5 (vertical)

[a] Tidal charts were obtained from the Hydro-Oceanographic Service of Indonesian Navy.
[b] Research Unit for Water Resources (UP-PSDA) of Syiah Kuala University in Banda Aceh.
[c] Faculty of Geo-information Science and Earth Observation (ITC), University of Twente in Enschede, The Netherlands.
[d] From an airborne survey conducted by the Norwegian Agency for Development Cooperation (NORAD) on behalf of the Survey and Mapping Agency of Indonesia (Bakosurtanal).
[e] Topographic contour derived from the basemap (3) by Japan International Cooperation Agency (JICA).
[f] Bureau of Rehabilitation and Reconstruction of Aceh and Nias (BRR Aceh–Nias).

complex of small dunes also characterized the pre-tsunami west coast, suggesting more than enough sediment supplied and deposited in this coastal environment. The foreshore slope was varying between 1:30 and 1:50. The shoreface slope was more or less the same as Ulee Lheue coast, nevertheless, it was connected to substantially wide inner shelf of 25 km width with average depth of −50 m. From here on, the slope breaks steeply into the inner shelf of −250 m depth (Fig. 1a).

The impact of the tsunami on the coastal morphology was revealed by the trim line of the stripped-off vegetation along the foot of the hills and promontories. The shore-parallel dune system along the northern part of the west coast was also cut back; some dunes were flattened and inlet mouths were eroded and widened. A considerable amount of coral reef debris was found at the beach opposite to the still intact fringing coral reefs (Fig. 1c).

2.2. Data overview

Data sets of different types (e.g. data points, contour lines, feature identifications from images and observational data) were used in this study (Table 1). As a result, each data set has a different character and quality. Aerial photos and satellite images are the main data sources used to identify shoreline changes and development. A mosaic of ortho-rectified aerial photo of Banda Aceh has the highest spatial resolution. The aerial photos were obtained nearly six months after the tsunami (i.e. 6 June 2005). The mosaic was resampled to a high spatial resolution raster image of 0.3 m pixel size. This map was used as the basemap for geo-referencing the other maps and satellite images being used for this study. The geo-reference details of the surveyed data are all transformed to the UTM zone 46 N and WGS 1984 ellipsoid datum.

The multi-spectral IKONOS satellite images used in this study consist of three bands which represent the red, green and blue. For feature extraction from satellite images, the colour images of such high-resolution provide detail clarity. To enhance this quality even more, a *user-defined* type of stretching for the three image bands was used. In this way, accuracy in terms of less supervision, less misinterpretation on the colour of the beach saturation level, as well as easily operational delineation process can be obtained.

The images were resampled to a spatial resolution of 2.5 m and then enhanced to improve the appearance of discernible coastal features. A coastal topographic contour map of Banda Aceh was derived from the ortho-rectified aerial photos (i.e. the base map) through a photogrammetric process. The contour line interval is 0.5 m, which facilitates a careful study of new developments along the coast.

Note that the bathymetric and coastal topographic data sets were only available for the upper shoreface zone from the three sets of surveys in 2001, 2006 and 2007 (Table 1 and Fig. 6a), and they cover only the northwest coast of Banda Aceh (i.e. Ulee Lheue). Therefore, analysis of coastal changes and development were focused on this particular zone. In addition, to utilize the images to delineate shorelines, the tidal stages at which the images were acquired must be known. The only available source for tides fluctuation in this region was the hourly tidal chart predictions released by the Hydro-Oceanographic Service of Indonesian Navy. All the elevation data references were transformed such that they became relative to the MLWL datum (where MLWL $= \pm 0.00$ m).

2.3. Raw data handling

Handling the raw data sets with different spatial and temporal dimensions constituted some challenges. To some extent, the procedure used to make the data compatible influences the methodology applied in this study.

High-resolution satellite images are typically expensive and only cover a small area. Consequently, the coverage of this type of data determines the spatial extent of the study locations. In order to generate a DEM, coastal topographic and bathymetric point data had to be integrated. Data gaps between coastal topography and bathymetry are common in this case and we therefore had to estimate elevation values to fill in these gaps. This was done by manual adjustments of bathymetric contours in the vicinity of a complicated coastal morphological feature.

2.4. Data uncertainty

Several uncertainties and errors may be present in the data. Vertical and horizontal errors in a bathymetric survey may originate from the equipment being used, i.e. due to the limited vertical accuracy of an echo sounder and the limitations of horizontal positioning equipment such as conventional geodetic equipment (e.g. theodolite and level), or GPS.

To estimate the horizontal deviations, the high-resolution base map was used to fix the position of the surveyed data (i.e. bathymetry and coastal topography). In the raw data for the bathymetry of 2006, we observed a linear shift of the horizontal position relative to the base map. This could be corrected by applying a simple horizontal

Fig. 1. Banda Aceh, northern tip of Sumatra Island, Indonesia. (a) Relief map depicting the low-lying Banda Aceh city and the sea shelf bathymetry (brown to white on the land part shows the low to high terrain elevation, the sea is shown in white with bathymetric contour). (b) Ulee Lheue at the northwest coast. (c) Lampu Uk at the west coast. Data source: (a) SRTM™ 2003, (c) IKONOS™ on 23 June 2004, (d) Quickbrid™ on 13 January 2002.

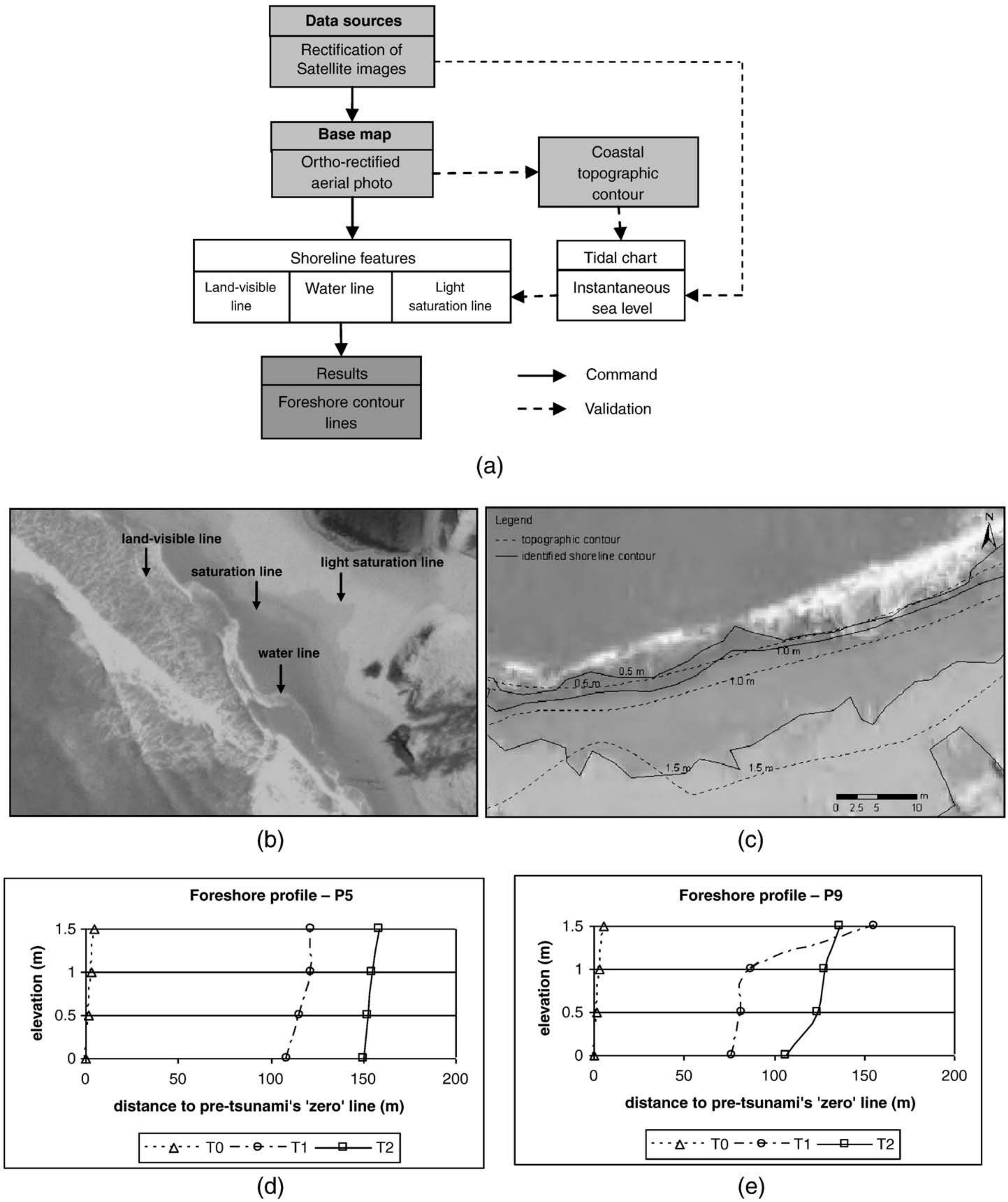

Fig. 2. Identification of multi-shoreline features. (a) Scheme of data source usage for multi-shoreline identification and its validation. (b) Multi-shoreline features. (c) Identified shoreline features in June 2005 on the west coast based on the contour map and discernible features, validated by the tidal chart. (d and e) Examples of foreshore slope of early and 6 months after the tsunami at Ulee Lheue Beach (profiles are depicted in Fig. 3a P7). Note: T0 = 23 June 2004, i.e. before the tsunami; T1 = 30 December 2004, i.e. 4 days after the tsunami; T2 = 6 June 2005, i.e. 6 months after the tsunami.

coordinate transformation. The 2007 data positions of the surveyed points had already been geometrically fixed. On the other hand, a slight rotational effect (about 10° due north) as compared to the overall position of the 2001 data was found. This problem was subsequently fixed by a rotation transformation operation. The remaining horizontal errors come from the shoreline delineation relative to the pixel size of the satellite images. All satellite images we used in this study have 2.5 m pixel size. The base map of 2005 has a pixel size of 0.3 m. When delineating the shorelines, the visual interpretation from the operator may have shifted to the neighbouring pixel, which error should be taken into account in the uncertainty analysis.

Another data error to be accounted is the vertical error. For 2001, the vertical uncertainty is associated with the accuracy of the echo sounder (i.e. ± 0.1 m) and the error on the level reading (i.e. estimated to be ± 0.1 m). In addition, the tidal records we used in this study were based on prediction based on tidal constituent analysis.

The Standard Root-Mean-Square Error (RMSE) procedure was used to calculate the horizontal and vertical uncertainties, e.g. as applied also by Rosati (2005) and Zhang et al. (2005) for similar sources of error. Hence, the RMSE of the vertical and horizontal uncertainties with respect to the multi-shoreline delineation are ± 0.14 m and ± 2.52 m, respectively.

3. Foreshore development study

This section presents the analysis of shoreline identification to quantify the changes and developments of the coastal morphology. The idea was to observe the coastal morphological response and short-term development (6 months) due to the earthquake and tsunami of the two coasts, which have different morphological characteristics.

3.1. Multi-shoreline identification

Identification of a ‘shoreline’ on the beach that is a repeatable, consistent, and meaningful indicator of sediment transport on the foreshore throughout time invites new interest and debate in the coastal scientific community (e.g. Ruggiero et al., 2003; Boak and Turner, 2005; Moore et al., 2006; and Farris and List, 2007), particularly since high-resolution satellite images and aerial photographs are increasingly utilized.

Two methods of identifying a ‘shoreline’ are defined by Moore et al. (2006); the visually proxy-based and the datum-based shoreline identifications. The visually proxy-based method typically identifies the landward extent of the last high tide and is recognized as a tonal contrast between the wet intertidal beach and the dry supratidal beach (Stafford, 1971; Dolan et al., 1978; Morton, 1979). Applying this method on the low resolution satellite images or topographic maps results merely a single shoreline. On the other hand, the usage of high-resolution images and aerial photo in this study enables the identification of multiple shorelines. The multiple shoreline definitions were adapted from the study by Boak and Turner (2005):

1) *Saturation line*, the border of the area which is saturated by groundwater (a similar feature was termed ‘groundwater exit point’ by Boak and Turner, 2005). The sand colour of this area is dark grey or dark brown, depending on the type of beach material.
2) *Light saturation line*, the border line of the previous run-up, which has less groundwater content than that of the *saturation line*. This is equal to MHWL in this study, which adapted the definition of the previous high tide water level by Boak and Turner (2005).
3) *Water line*, the border line of the instantaneous water body, which appears in green or blue.
4) *Land-visible line*, the border line of the water body where the submerged land just below the water is still visible.

The datum-based shoreline is derived from topographic surveys (Smith and Zarillo, 1990; Ruggiero et al., 2003; Farris and List, 2007) or laser altimetry data are based on the cross-shore position of an elevation contour extracted from topography. We combined these two methods in this study to be able to determine the elevations of the multiple shorelines which initially have no elevation information from the satellite images. Thus, a coastal topographic map was used to give approximate elevation to the multiple shorelines, which actually creates contours of the foreshore zone morphology. A tidal chart associated with the time at which the satellite image was acquired was used to validate the water level position in that image (schematized procedure in Fig. 2a).

The elevation of each shoreline in this case was determined by correlating its position to the topographic contour lines and the corresponding tidal stage. As an example of this procedure, Fig. 2b shows the identified shorelines of the Lampu Uk foreshore (between profiles P1 and P2 in Fig. 4b). Similar identification was carried out at Ulee Lheue foreshore in Fig. 2c which shows that the contour of $+1.5$ m coincided with the landward edge of the light saturation zone, which was therefore determined as the light saturation line. The tidal chart confirmed this elevation of $+1.5$ m as well, which was actually the Mean High Water Level (MHWL) position of the tidal range. This led to the first estimate that the light saturation line appeared in the particular satellite image can be identified as MHWL. Knowing that the $+1.5$ m contour corresponds to MHWL, the other contour lines from the coastal topographic map can be used to estimate the other coastal features' elevations.

Hence, from the four shoreline features, there were only three that can be used to estimate elevation: i) the light saturation line (elevation $+1.5$ m); ii) the water line (elevation $+1.0$ m); and iii) the land-visible line (elevation $+0.5$ m). From these data, the shoreline position as well as the steepness of the foreshore slope change over time can be observed. Having the positions of the $+0.5$, $+1.0$ and $+1.5$ m contours, it was assumed that the position of the ± 0.00 m contour line can be obtained by linear extension of the slope of the foreshore zone.

It is more convenient to measure the total uncertainty of the resulting horizontal distance of one shoreline feature to the other in a single satellite image being used (e.g. between $+0.5$ m and $+1.0$ m shorelines of image acquired on 30 December 2004). We calculated that the minimum and maximum distances created from the shoreline delineation in total are 1.3 ± 2.52 m and 46.9 ± 2.52 m for Ulee Lheue coast, and 0.78 ± 2.52 m and 10.23 ± 2.52 m for Lampu Uk coast.

With regard to the above-mentioned multiple shoreline definitions, we minimized the horizontal uncertainty from the human error during the shoreline delineation by maintaining the consistency of the delineation of each defined shoreline features (i.e. saturation, light saturation, water and land-visible lines) with the associated topographic contour lines derived from the photogrammetry and the predicted tidal stage. To check the consistency, the aerial photo mosaic and the other satellite images of the coastal stretches with a gentler beach slope (wider beach) along the northwest and west coasts were examined in the same way. It appeared that even though the colour tones of the coasts may be quite different, the shoreline features were similarly discernible. As a matter of fact, each image that was acquired at a different tidal stage helps to improve the elevation of shoreline approximation.

3.2. Quantification of sediment volume changes in the foreshore zone

Changes of shoreline position between images from different points in time show visually the impact and the development of the

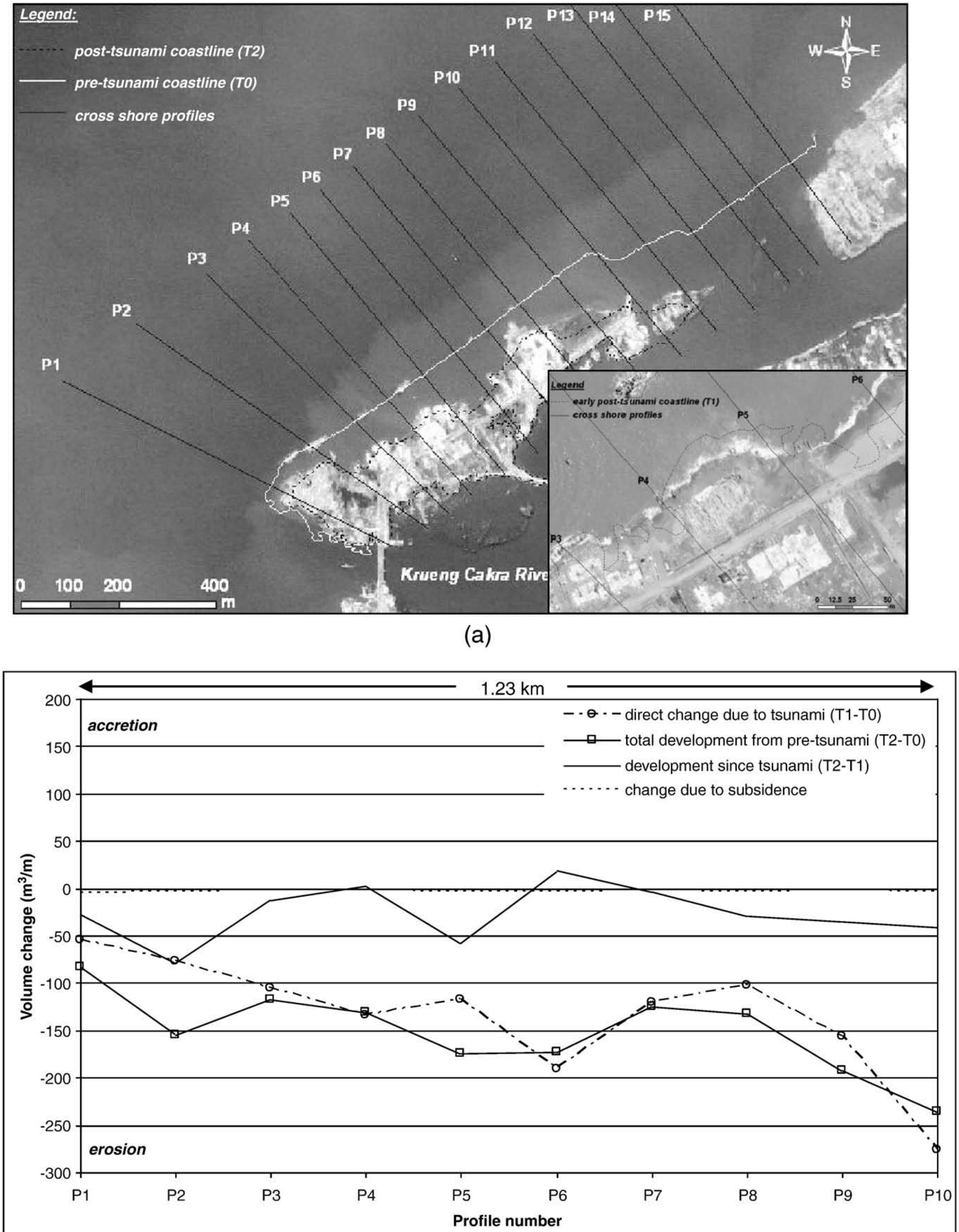
Legend:
post-tsunami coastline (T2)
pre-tsunami coastline (T0)
cross shore profiles
P1
P2
P3
P4
P5
P6
P7
P8
P9
P10
P11
P12
P13
P14
P15
N
W
E
S
Krueng Cakra Rive
0 100 200 400
m
Legend
early post-tsunami coastline (T1)
cross shore profiles
1.23 km
accretion
erosion
direct change due to tsunami (T1-T0)
total development from pre-tsunami (T2-T0)
development since tsunami (T2-T1)
change due to subsidence
Volume change (m3/m)
200
150
100
50
0
-50
-100
-150
-200
-250
-300
Profile number

(a)

(b)

coastal morphology since the tsunami. The subsequent step was to quantify the magnitude of those changes. A simple volumetric control principle was adopted to calculate the amount of sediment loss or gain from two consecutive coastal profiles. Fig. 2d and e shows the foreshore profiles (derived from the elevations of the shoreline features) for two locations at 3 instants in time.

The pre-tsunami 0.00 m contour position was used as the reference to measure the distance between the consecutive shoreline positions (i.e. T1–T0 and T2–T0 in Fig. 2d and e). The distances between the pre- and the early post-tsunami profiles (T1–T0) and between the pre- and 6 months post-tsunami profiles (T2–T0) were determined to calculate the volume of sediment erosion or deposition in m^3/m. Subsequently, the difference between the two calculated volumes determines the volume change due to the morphological development in the foreshore zone since the tsunami (T2–T1).

3.2.1. Ulee Lheue, northwest coast

Satellite images acquired directly after the tsunami display severe coastline retreat at Ulee Lheue as a direct impact of tsunami waves and/or subsidence. The images show the presence of a chaotic shoreline, a destroyed seawall and a severely eroded and breached beach ridge (comparing Figs. 1b and 3a). Most of the profiles along the Ulee Lheue foreshore revealed significant erosion (i.e. T1–T0 in Fig. 3a).

In the first 6 months after the tsunami, the new surf zone (recognized by the position of the breaking wave line) was reshaped. The shoreline became less undulating, and the foreshore zone tended to shift landward. Littoral sediment appeared to have been re-distributed alongshore, as revealed by the accretion at profiles P4 and P6, and the smoothed edge of pointed remnants (between P7 and P8) adjacent to them (see shoreline positions in Fig. 3a). The remnants of the breached beach ridge such as those between P9 and P11 started to re-connect by the building up of new beaches from fresh sediment deposits to a level comparable to MHWL (+1.5 m).

As a result of the tsunami, the shorelines retreated on average about 73 ± 2.52 m from the pre-tsunami position. This is comparable to a total volume of sediment loss in the initial response to the tsunami (T1–T0 in Fig. 3b) of 2.6×10^3 m^3/m.

In the following 6 months, or two months after the second big earthquake in March 2005, the shoreline continued to retreat, resulting in an average distance of 84 ± 2.52 m from the pre-tsunami shoreline. This is comparable to the amount of a total volume of sediment loss of 3.0×10^3 m^3/m (i.e. T2–T0 in Fig. 3b). This implies that ongoing retreat occurred during the 6-month development, which equals about 15% (0.4×10^3 m^3/m) of the sediment loss due to the tsunami (i.e. T2–T1 in Fig. 3b).

3.2.2. Lampu Uk, west coast

The morphological response to the tsunami on the west coast, represented by Lampu Uk beach, was similar to the northwest coast, i.e. chaotic shorelines. Beach scouring by the strong waves created depressions, which were commonly found along the coast (i.e. inland water bodies in the vicinity of profiles P8–P10 and P19–P20 in Fig. 4a).

The Lampu Uk shoreline along profiles P1 to P21 significantly retreated on average as far as 77 m landward from the pre-tsunami's shoreline, while the adjacent part, i.e. P22–P27, retreated less. The coastal section P1–P21 was a non-protected sandy beach with a gentle slope, while the adjacent coastal section in the south was a beach with dune formation with a maximum elevation of ca. 10 m above MLWL. Coastal protection structures such as the beach revetment along profile P25 to P27 may have helped the southern coastal section survive the tsunami. As a matter of fact, during the field visit in May 2005, we observed that the she-oak trees (*Casuarina equisetifolia*) behind this section survived the tsunami, and the beach revetment in front of them was still intact.

In the 6 months after the tsunami, the Lampu Uk shoreline significantly advanced seaward along the entire north part (P1–P21), which contrasted with a slightly retreating shoreline further south (P22–P27). This accretion phenomenon was considerably different from what has occurred on the northwest coastal section (Ulee Lheue).

Prior to the tsunami, small inlets of profiles P8 and P10 were once inland depressions. During the tsunami, the beach in front of them was breached and this connected the depressions to the sea. The beach in the vicinity was also flattened and massive coral reef debris was dumped on the beach, which likely originated from the fringing coral reef complex in front of the small promontory (profiles P10–P20). The development of the promontory showed a significant beach growth orientated northwards, suggesting the prevailing direction of the longshore sediment transport of this region. A newly formed inlet between profiles P16 and P17 remained open, indicating that the tidal currents were strong enough to prevent the inlet from closing, even though the adjacent beach kept accreting.

The total amount of sediment loss due to the tsunami and the sediment gain during the subsequent development were 4.0×10^3 m^3/m and 1.6×10^3 m^3/m, respectively (Fig. 4b). This means that 2.2×10^3 m^3/m or about 60% of the sediment loss due to the tsunami was gained back into the beach stretch within 6 months.

3.3. Observations on land subsidence

Evidences of land subsidence were obtained in this study by comparing the two photographs of coastal structures at the same location and two beach profile elevations of pre- and post-tsunami situations derived from the DEM 2001 and DEM 2006 at Ulee Lheue. Fig. 5a shows the remnant of Ulee Lheue beach as seen from the bridge, facing seaward on 21 January 2005 (after the earthquake of December 2004) during the low tide level at +0.0 m from MLWL. Fig. 5b shows the same location on 12 April 2005 (after the earthquake of March 2005) during the rising tide at +0.6 m from MLWL. Knowing that the elevation of the coastal structure remnants in Fig. 5a was about +1.8 m from MLWL, and of the remnants in Fig. 5b about +0.6 m from MLWL, the subsidence of the location was estimated at about 0.6 m.

Comparable estimates of land subsidence magnitude in both coasts were described earlier by some other authors. A near-field geodetic measurement combined with satellite images and a tidal model by Subarya et al. (2006) revealed the detectable range of land subsidence near Ulee Lheue and Lampu Uk as 0.0 to −1.0 m. Meltzner et al. (2006) estimated the constraint of land subsidence near Ulee Lheue coast from satellite images within the range of 0.1 to 0.2 m. Furthermore, Jaffe et al. (2006) suggested that the land subsidence near Lampu Uk was as low as 2.0 m.

We expected that this *a priori* information about the land subsidence would contribute to a better analysis of the observed coastal morphological development after the earthquake and tsunami events. The quantification of the sediment loss due to land subsidence was done by taking into account the slope of each foreshore profiles obtained from the multiple shoreline analysis and the subsidence heights estimated at each coasts from the field observations. Figs. 3b and 4b show the results of the quantification of the sediment loss due to the land subsidence for Ulee Lheue and Lampu Uk, respectively.

Fig. 3. (a) Examples of shoreline contours (+0.5 m) and sediment volume changes at Ulee Lheue beach. The background image showing the situation directly after the tsunami (T1). The development after 6 months is shown by the black dashed line. The inset figure shows the situation 6 months after the tsunami (T2) which reveals a new surf zone with apparent breaking wave pattern. On top of that, the dashed line represents the shoreline directly after the tsunami (T1). Image source details are shown in Table 1. (b) Sediment volume change in m^3/m along the Ulee Lheue coast. Note: T0 = 13 January 2003; T1 = 30 December 2004; T2 = 6 June 2005.

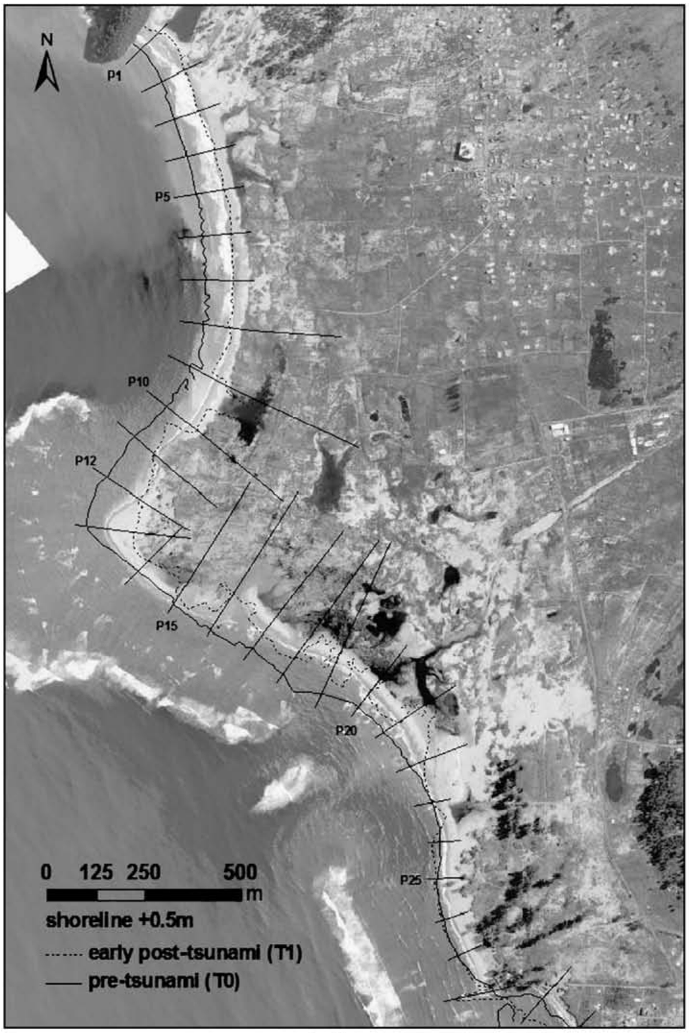
N
P1
P5
P10
P12
P15
P20
P25
0 125 250 500
m
shoreline +0.5m
early post-tsunami (T1)
pre-tsunami (T0)

(a)

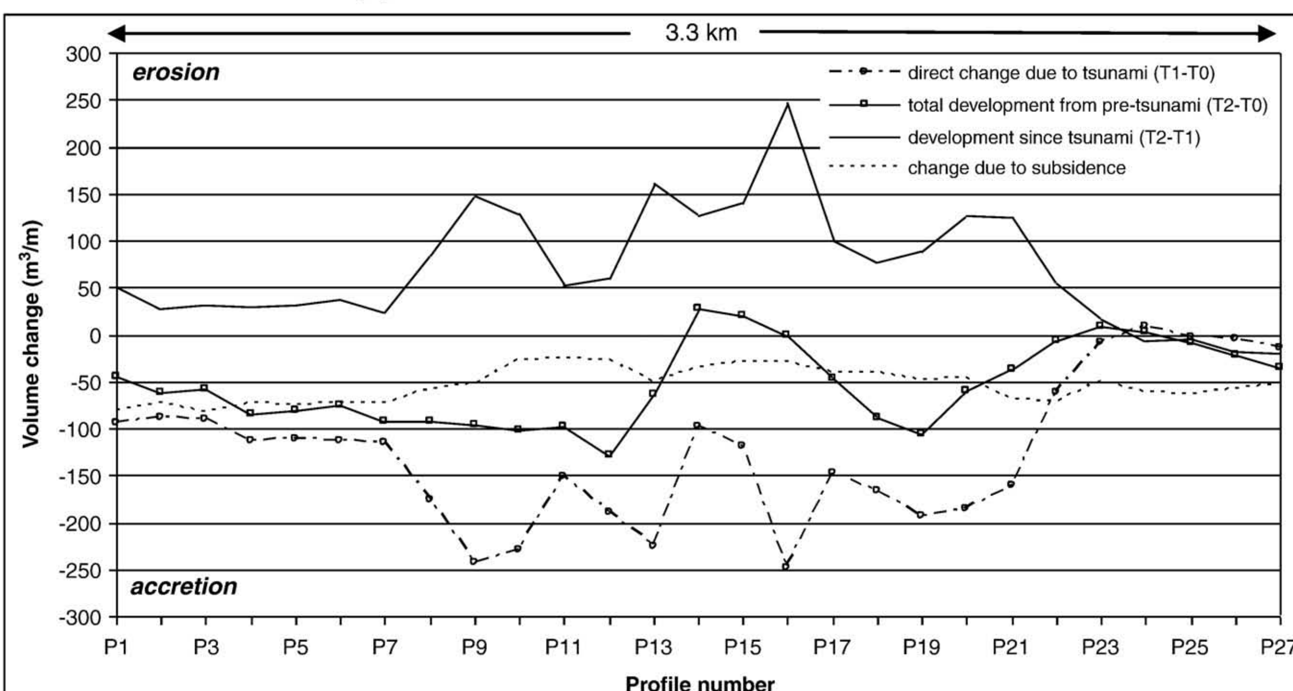
3.3 km
erosion
accretion
direct change due to tsunami (T1-T0)
total development from pre-tsunami (T2-T0)
development since tsunami (T2-T1)
change due to subsidence
Volume change (m3/m)
300
250
200
150
100
50
0
-50
-100
-150
-200
-250
-300
P1
P3
P5
P7
P9
P11
P13
P15
P17
P19
P21
P23
P25
P27
Profile number

(b)

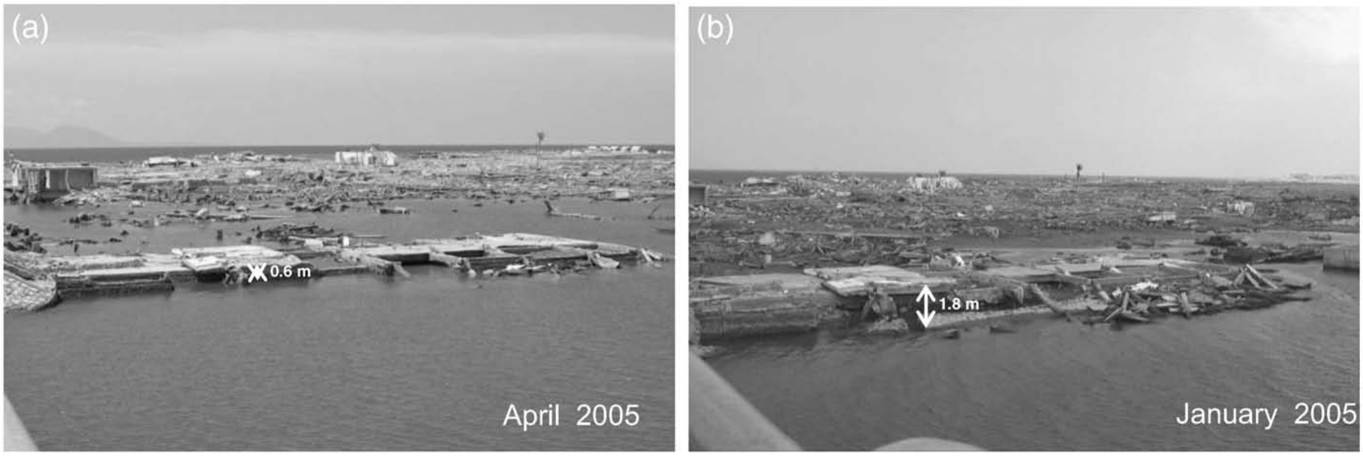

Fig. 5. Evidence of land subsidence from the coastal building remnants on the back-barrier of Ulee Lheue coast, which reveal vertical changes relative to sea level. (a) On 21 January 2005 during the low tide (+0.0 m); (b) on 12 April 2005 (after the great earthquake on 28 March 2005) during the rising tide (+0.6 m). Further description is in Section 3.3.

4. Digital Elevation Models (DEMs) of shoreface development at Ulee Lheue

Up to this point, the quantification of morphological development of the foreshore zone has given an idea of how much sediment exchange took place in the foreshore zone in the short period since the earthquake and tsunami. In this section, the study is expanded to a larger area of coastal zone, covering the shoreface, foreshore and backshore at Ulee Lheue. Three-dimensional morphological changes and developments were studied by using coastal profiles normal to the coastline. The morphological pattern development over time can be determined from changes in elevation of two consecutive coastal profiles, i.e. 2001–2006 and 2006–2007, shown in Fig. 6c. Sediment volume changes (i.e. erosion, deposition and net change) are also quantified in this section.

4.1. Input data and methods

Different data sources, in terms of topography and bathymetry, were compiled as input to generate a DEM. In this study, three sets of bathymetric–topographic integrated data sets were used: i) pre-tsunami data of April 2001; ii) one year post-tsunami data of January 2006; and iii) two-year post-tsunami data of January 2007 (see also Table 1). The bathymetry of 2006 and 2007, measured during the month of January of the corresponding year, gave an opportunity to observe seasonal morphological development after a full cycle of monsoonal climate.

For this study, a DEM was generated using the Triangulation Irregular Network (TIN) method. The TIN is an interpolation method which facilitates integration of several data types, for example, a segment (contour) map combined with a point elevation map. The result of this process is a surface map configured by the triangular nodes obtained from the interpolation process. The first DEM generation may yield unreliable contours at a certain location during the interpolation. Therefore, an adjustment process had to be carried out subsequently. The degree of reliability depends very much on the data density. The greater the distance between one data point and another, the larger the uncertainty. Fig. 6a shows the bathymetric data points from the measurements conducted in front of the Ulee Lheue coast in 2001, 2006 and 2007 used in this study. After generating the initial DEM, a contour line map with a 0.5 m contour interval was extracted.

4.2. Morphological development of the shoreface

Fig. 6b shows the results of DEMs generation from three consecutive data of pre-tsunami (2001), one year post-tsunami (2006) and two-year post-tsunami (2007). The colour gradation from red to blue represents the sub-aerial to sub-aqueous part of the coastal area.

The shoreface profiles were subsequently extracted from the DEM as depicted in Fig. 6c. Profile P1 consisted of a set of submerged ebb-tide delta lobes deflected seaward at the northeast side of the Krueng Cangkoy river mouth (see DEM 2001 in Fig. 6b). Furthermore, the data show a trench complex, situated in the middle of the coastal section (between P5 and P7 in Fig. 3a or the dark blue portion near P5 of DEM 2001 in Fig. 6b). A gentle shoreface profile was observed in the northeast section (P10 to P15) which used to be an open beach. The shoal across profile P1 existed since the past century after the southwest-end portion of the beach ridge was breached in early 1900s (see Meilianda, 2009).

4.2.1. Morphological development till 1 year after the tsunami (2001–2006)

From the plan view depicted in Fig. 6b, after one year development in 2006, the morphology shows an irregular surface pattern with prominent shoals and troughs. A significant change from the pre-tsunami morphology is revealed by the partially-removed shoal near profile P1, filling-up the trench complex in the middle section near profile P5 and the rebuilt beach at the northeast (near profiles P10 and P15).

Four representative profiles of P1, P5, P10 and P15 showed that the area under consideration had been dynamically modified by the tsunami. The filling-up of the trench near profile P5 with an enormous amount of supplied sediments have occurred as the immediate response to the multiple incoming tsunami wave action (i.e. three consecutive waves according to Paris et al., 2007). The deposited amount of sediment in the trench complex was higher than the amount of sediment erosion on the associated foreshore. Profile P15 represents the least artificially modified coastal stretch. Here, it can be

Fig. 4. (a) Examples of shoreline changes (contour +0.5 m) and sediment volume changes at Lampu Uk. The background ortho-rectified aerial photo shows the development of the coast in June 2005 (6 months after the tsunami). (b) Sediment volume change along the foreshore zone. Note: T0 = 13 January 2003; T1 = 30 December 2004; T2 = 6 June 2005.

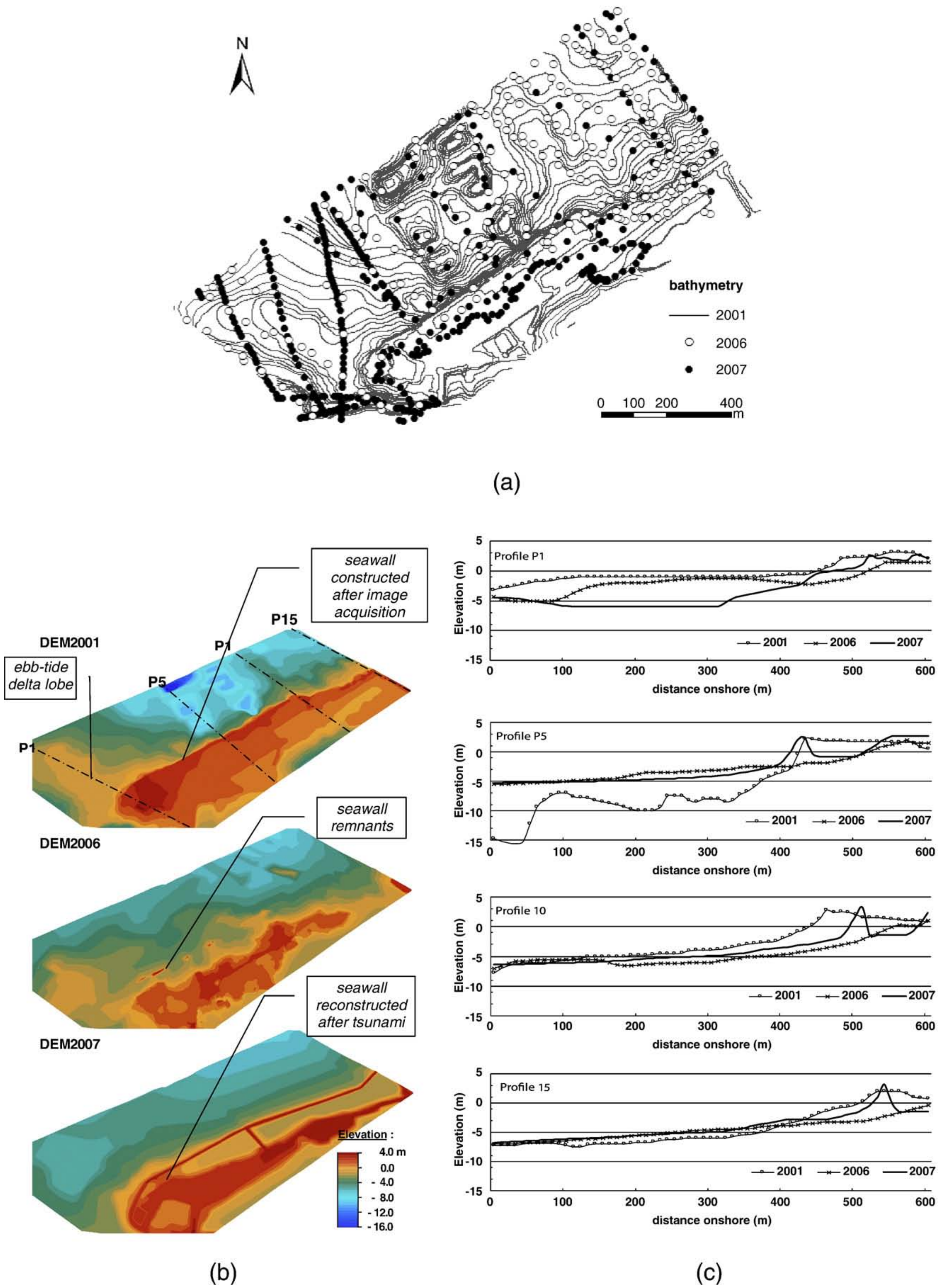

Fig. 6. Digital Elevation Model (DEM) for Ulee Lheue coast. (a) Bathymetric data type and density from the survey conducted in 2001, 2006 and 2007. (b) Generated DEMs of Ulee Lheue coast derived from bathymetric measurements datasets. (c) Four representative coastal profiles describing the morphological development in time along the coast which were derived from the three sets of DEM.

Table 2
Sediment volume change at Ulee Lheue (in 10^3 m^3).

Period	Erosion	Deposition	Net change	Note
2001–2006	716	924	208	Accreting
2006–2007	614	397	−217	Eroding

observed that the difference between foreshore and backshore erosion and shoreface accretion was small. Profile P10 shows significant erosion both in the shoreface and foreshore zone.

Overall, in this early development period of the coastal morphology, the sediment re-distributed in such a way that foreshore and backshore erosion coincided with shoreface accretion in most profiles, except in the northeast region (P10), where a significant amount of deposition occurred both on the shoreface and foreshore.

4.2.2. Morphological development till 2 years after the tsunami (2006–2007)

The shoreline change study in Section 3 revealed that the pre-tsunami beach disappeared as an early response to the earthquake and tsunami, and a new beach developed further landward. Note that as a means of inland protection from further shoreline retreat, a new seawall was built between August 2006 (near profile P1) and December 2006 (near P10), along the new position of the shoreline.

The DEM 2007 shows that the shoal at the southwest near P1 has completely been removed and the shoreface morphology towards the middle and the northeast subregion (i.e. from P5 to P15) became smoother compared to the earlier development (DEM 2006). Fig. 6b and c reveals that since 2006, the sediments seem to have been further re-distributed along the entire shoreface.

The flattened shoal near P1 is an apparent striking phenomenon in this case. Nevertheless, no readily explanation so far about this phenomenon since up to this point our analysis was solely depending on bathymetric data. As far as we understood it has nothing to do with natural processes. In conjunction with the new seawall construction (see DEM 2007 in Fig. 6b), there was coastal reclamation activity to re-connect Ulee Lheue to the Ferry Port, in which most of the material was taken from the lobe.

There were slight erosion in the shoreface of P5, deposition in the shoreface of P10, and almost no change in the shoreface of P15. This recent development of the shoreface shows that the shoreface profile was developing towards the pre-tsunami slope gradient, two years after the tsunami.

A summary of the total volume change in m^3 by subtracting two pairs of consecutive DEMs is displayed in Table 2. Note that this analysis does not discriminate erosion/deposition and net changes to the shoreface and foreshore. One year after the tsunami (2006), the net sediment volume change reveals significant sediment input to the shoreface, while the foreshore zone experienced severe erosion. In the following year (2007), the sediment went out of the coastal section as the shoreface bed became smooth.

5. Discussion

In general, chaotic shoreline undulations created by the tsunami along the northeast and west coasts of Banda Aceh developed into less undulating shorelines several months after the tsunami. Both coasts showed chaotic shorelines as the response to the tsunami waves. Before the tsunami, the surf zone of the northwest coast and the west coast were usually extended on average about 10 m and 20 m seaward of the water line, respectively. As the wave climate returned to normal after the event, the new foreshore on both coasts should have had similar surfzone widths. Nevertheless, four days after the tsunami, the wave breaking lines of both coasts were situated very close to the water line. Fig. 3a shows that the surfzone widths of both coasts were narrower in the early days after the tsunami, which suggests that the foreshore was out of the equilibrium.

Subsequently, the coasts experienced a morphological adjustment process. Within 6 months, the shoreline undulations of both coasts were gradually decreasing and the foreshore slope became straighter. Although this morphological adjustment occurred on both coasts, i.e. Ulee Lheue and Lampu Uk, interestingly, they developed in opposite trends from their pre-tsunami positions. Ulee Lheue, on the northwest coast, experienced ongoing erosion of about 15% of the total sediment loss due to the tsunami; Lampu Uk on the west coast gained back 60% of the sediment loss due to the tsunami after 6 months. These numbers were derived from the sediment volume changes in the foreshore zone displayed in Figs. 3b and 4b.

In the following sections, the analysis of short-term morphological development since the earthquake and tsunami of the two coasts with different geomorphic settings will be discussed. Aspects such as the land subsidence, geomorphic settings and sediment availability in the coastal system of the two different coasts that are influencing the short-term coastal development are considered.

5.1. The influence of land subsidence and tsunami on a sand-poor environment

As was described in Section 2.1.1, the northwest coast Ulee Lheue is typically a sand-poor coastal environment and is not significantly influenced by the sediment supply from a river. It also has a narrow and steep inner shelf. As the offshore sea bed of the northwest coast was plunging to a depth of over 200 m from the slope break, some sediment which was re-distributed during the tsunami may have been deposited in the deep offshore. Also, according to observations from several earlier studies (Gibbons and Gelfenbaum, 2005; Dohmen-Janssen et al., 2006; Jaffe et al., 2006; Paris et al., 2007) sediment was deposited inland. Much of the sediment may never return to the shoreface as the influence of the waves was considerably less at the offshore and inland deposits may have been settled or consolidated. Therefore, we expect a shortage of temporary sediment storage within the shoreface (e.g. the bumpy surface in DEM 2006 in Fig. 6b).

The prevailing recovery process after the tsunami in the littoral zone was, therefore, the re-organization of the shoreline by littoral transport which once was highly modified (chaotic) by the tsunami waves. As was observed during the field visit in June 2005 and also in Figs. 3a and 4a, the shoreline becomes more regular. At the same time though, the foreshore tent to be further eroded in such a way it undergoes a self-feeding sediment transport mechanism. From this point on, the recovery process might have been slowed down. Since seasonal change was not important in this particular coastal section, we assumed that the foreshore morphology from June 2005 until January 2006 was steady.

Fig. 3b shows the erosion effect from the land subsidence, which is apparently not to be dominant in this coast, compared to the erosion that was caused by the tsunami waves. Nevertheless, the graph also displayed the ongoing erosion occurred during the first 6 months of the morphological development in front of this particular coast. Also, keeping in mind that this coast is a sand-poor environment with relatively narrow and steep shoreface, this suggests that the short-term regular coastal process could not keep pace with not only the sudden loss of sediment due to land subsidence, but also to a greater extent, due to lack of sediment availability in the coastal system to replace the amount of sediment loss due to the tsunami waves.

5.2. The influence of land subsidence and tsunami on a sand-rich environment

As was described in Section 2.1.2, Lampu Uk on the west coast of Banda Aceh is a sand-rich coastal environment with a considerably wider inner shelf compared to Ulee Lheue on the northwest coast. Fig. 4b displays sediment erosion and accretion on the foreshore zone which are substantially different, both in the course of land subsidence and tsunami, from those occurred at Ulee Lheue.

The sediment loss due to land subsidence here is higher compared to that of Ulee Lheue. Severe erosion occurred particularly at profiles P9, P13, P16 and P19 (Fig. 4b). Nevertheless, in the subsequent 6 months, the development shows significant accretion at almost the entire coastal stretch (T2–T1 line in Fig. 4b). This suggests that there has been a substantial regaining amount of sediments on the west coast. It compensated to a great extent the sudden loss of sediments due to land subsidence (comparing the T2–T0 and the subsidence lines in Fig. 4b). We argue that the accretion was associated with the amount of sediments that were temporary stored somewhere within the coastal system. The wide and shallow inner shelf and higher wave energy in this coastal region can be the controlling factor of this temporary sediment storage and the rapid accretion.

Furthermore, during the field visit on the west coast in August 2006, it was observed that the tsunami-related scours on the beach (backshore) were filled in with thick sand deposits and the beach was more elevated than previously observed. As the result of the erosion combined with the land subsidence, after the tsunami, a sand-rich coast tend to recover by shifting the foreshore landward and rapidly accumulate the amount of sand on top of the old backshore. This accretion somehow created a problem for the inhabitants because the existing coastal road was gradually overtopped by sand.

Such foreshore recovery stages during the first nearly-two years (December 2004 to August 2006) were comparable to that of the sand-rich southeastern Texas coast, USA after the Alicia, a category-3 hurricane with a storm surge of over 3.9 m, providing the scale of the event is different from that of the tsunami (tsunami waves were recorded to be 10 m high in Lampu Uk). Within two years aftermath, Morton et al. (1994) examined that after the Alicia, the first stage of foreshore response lasted about one year, and involved shoreward sand migration, foreshore deposition, and rapid advancement of the berm crest. This was followed by the second stage where sediments of the aggrading berm crest were eroded by high waves (during hurricane) which transported them landward, thereby aggrading the backshore near the post-storm erosional escarpment. From the two stages, the new beach material will be imprinted as the unconformable geological strata to understand the occurrence of such extreme event at the particular coast in history (e.g. when a core sample would be taken on the site).

Overall, the stages of recovery process of a coast affected by a tsunami are comparable to that affected by a hurricane; it experienced initial rapid adjustment of the foreshore slope and shoreline undulations, and subsequently followed longer period of shoreface re-organization into a smoother surface. Moreover, the type of geomorphic settings (e.g. foreshore slope and the shoreface and inner shelf width and their geological deposits), the aftermath sediment characteristics and availability (sand-poor or sand-rich coastal environment) as well as the magnitude of the land subsidence determine the trend of morphological development of the coast after the tsunami. This analysis expands the horizon of understanding the role of geomorphic settings to the sediment deposition and re-distribution by the tsunami waves from several field observations which were previously conducted at different locations by Umitsu et al. (2007), Narayana et al. (2007), and Gibbons and Gelfenbaum (2005).

6. Conclusions

A combination of satellite images, topographic and bathymetric data from different sources and from multiple years was used in this study to observe the changes and development of two tsunami-affected coastal sections near Banda Aceh; a sand-poor northwest coast Ulee Lheue and a sand-rich west coast Lampu Uk. The data covered a small spatial scale (approximately 1 to 3 km) the two coasts. An attempt to integrate several available data sources led to the selection of the following methods: i) multi-shoreline identification in the foreshore zone; and ii) multi-temporal DEMs in the foreshore and shoreface. This data-driven analysis explores the utmost usefulness of the multi-source data and field observations to answer the main research question in this study, which is on how the coast developed after the tsunami on a relatively short time scale.

After 6 months development, the two coasts developed towards a contrasting behaviour. Ulee Lheue on the northwest coast experienced ongoing erosion of about 15% of the total sediment loss due to the tsunami, while 60% of that on the west coast (Lampu Uk) was compensated for accretion.

We expect a shortage of temporary sediment storage occurred within the shoreface of Ulee Lheue six months after the tsunami, keeping in mind that this coast is a sand-poor environment with relatively narrow and steep shoreface. The ongoing erosion on the foreshore suggests that the short-term regular coastal process could not keep pace with not only the sudden loss of sediment due to land subsidence, but also to a greater extent, due to lack of sediment availability in the coastal system to replace the amount of sediment loss due to the tsunami waves.

We argue that the accretion on the west coast was associated with the amount of sediments that were temporary stored somewhere within the coastal system. The wide and shallow inner shelf and higher wave energy in this coastal region can be the controlling factor of this temporary sediment storage and the rapid accretion. Moreover, a substantial regaining amount of sediments occurred six months after the tsunami. It compensated to a great extent the sudden loss of sediments due to land subsidence which was greater than the one on the northwest coast.

This study confirms our hypothesis on the morphological response and the subsequent morphological development of a coast after the large scale earthquake and tsunami. The extent of the impact depends on the geomorphic settings inherited to the coast. The subsequent morphological development is determined by the extent of the impact itself, the geomorphic settings of the coast in which the sediment re-distributed and the available sediment that are movable by the normal wave condition after the tsunami event.

Acknowledgements

We address our acknowledgement to UP-PSDA Hydraulic Laboratory of Syiah Kuala University for providing the bathymetry and topography data of 2001, to Bakosurtanal through the SIM-center BRR NAD Nias in providing the ortho-rectified aerial photo mosaic and to the Sea Defence Consortium — BRR Aceh–Nias for providing the bathymetry, topography and other supporting data of 2006 and 2007. We also address our thanks to Dr. Kathelijne Wijnberg from the University of Twente for her constructive comments to the completion of this manuscript, Dr. Guy Gelfenbaum from US Geological Survey for sharing information on his fieldwork findings of the land subsidence and to Dr. Poh Poh Wong from National University of Singapore for collaborations during the two field observations. This study is funded by the Asian Development Bank (ADB) through the TPSDP Project of the Higher Education Department of Republic of Indonesia.

References

Anonymous, 1997. Report on oceanography parameter measurements and wave analysis. Detail design of beach revetment of Lampu Uk beach, Great Aceh. Western coastal safety project, Civil Work Department, Aceh Province, Banda Aceh.

Boak, E.H., Turner, I.L., 2005. Shoreline definition and detection: a review. Journal of Coastal Research 21 (4), 688–703.

CERC, 1992. Automated Coastal Engineering System, Volume I: Technical Reference; Vol II: User's Guide, Department of the Army Water-way Experiment Station, Corps of Engineers, Mississippi.
Dohmen-Janssen, C.M., Meilianda, E., Maathuis, B.H.P., Wong, P.P., 2006. State of Banda Aceh beach before and after the tsunami. Proceeding of 30th International Conference on Coastal Engineering. ASCE, San Diego, California.
Dolan, R., Hayden, B., Heywood, J., 1978. A new photogrammetric method for determining shoreline erosion. Coastal Engineering 2, 21–39.
Farris, A.S., List, J.H., 2007. Shoreline change as a proxy for subaerial beach volume change. Journal of Coastal Research 23 (3), 740–748.
Gelfenbaum, G., Jaffe, B., 2003. Erosion and sedimentation from the 17 July 1998 Papua New Guinea tsunami. Pure and Applied Geophysics 160 (10–11), 1969–1999.
Gibbons, H., Gelfenbaum, G., 2005. Astonishing wave heights among the findings of an international tsunami survey team on Sumatra. Sound Waves March 2005 (monthly newsletter). http://soundwaves.usgs.gov/2005/03/2005.
Jaffe, B.E., Borrero, J.C., Prasetya, G.S., Peters, R., McAdoo, B., Gelfenbaum, G., Morton, R., Ruggiero, P., Higman, B., Dengler, L., Hidayat, R., Kingsley, E., Kongko, W., Lukijanto, Moore, A., Titov, V., Yulianto, E., 2006. Northwest Sumatra and offshore islands field survey after the December 2004 Indian Ocean tsunami. Earthquake Spectra 22 (S3), 105–135.
Meilianda, E., 2009. Past, present and future morphological development of a tsunami-affected coast. Ph D Thesis, University of Twente, the Netherlands, 188pp.
Meltzner, A.J., Sieh, K., Abrams, M., Agnew, D.C., Hudnut, K.W., Avouac, J., Natawidjaja, D.H., 2006. Uplift and subsidence associated with the great Aceh–Andaman earthquake of 2004. Journal of Geophysical Research 111, B02407.
Moore, L.J., Ruggiero, P., List, J.H., 2006. Comparing mean high water and high water line shorelines: should proxy-datum offsets be incorporated into shoreline change analysis? Journal of Coastal Research 22 (4), 894–905.
Morton, R.A., 1979. Temporal and spatial variations in shoreline changes and their implications, examples from the Texas Gulf Coast. In: Moore, L.J., Ruggiero, P., List, J.H., 2006. Comparing mean high water and high water line shorelines: should proxy-datum offsets be incorporated into shoreline change analysis? Journal of Coastal Research 22(4), 894–905.
Morton, R.A., Paine, J.G., Gibeaut, J.C., 1994. Stages and durations of post-storm recovery, southeastern Texas coast, USA. Journal of Coastal Research 10, 214–226.
Narayana, A.C., Tatavarti, R., Shinu, N., Subeer, A., 2007. Tsunami of December 26, 2004 on the southwest coast of India: post-tsunami geomorphic and sediment characteristics. Marine Geology 242, 155–168.
Noda, A., Katayama, H., Sagayama, T., Suga, K., Uchida, Y., Satake, K., Abe, K., Okamura, Y., 2007. Evaluation of tsunami impacts on shallow marine sediments: an example from the tsunami caused by the 2003 Tokachi-oki earthquake, northern Japan. Sedimentary Geology 200 (3–4), 314–327.
Paris, R., Lavigne, F., Wassmer, P., Sartohadi, J., 2007. Coastal sedimentation associated with the December 26, 2004 tsunami in Lhok Nga, west Banda Aceh (Sumatra, Indonesia). Marine Geology 238, 93–106.
Rosati, J.D., 2005. Concepts in sediment budgets. Journal of Coastal Research 21 (2), 307–322.
Ruggiero, P., Kaminsky, G.M., Gelfenbaum, G., 2003. Linking proxy-based and datum-based shorelines on high-energy coastlines: implications for shoreline change analyses. Journal of Coastal Research SI-38, 57–82.
Sallenger, A., Wright, C.W., Lillycrop, J., 2007. Coastal-change impacts during Hurricane Katrina: an overview. Proceeding of the 6th International Symposium on Coastal Engineering and Science of Coastal Sediment Processes. ASCE, New Orleans, Louisiana.
Smith, G.L., Zarillo, G.A., 1990. Calculating long-term shoreline recession rates using aerial photo-graphic and beach profiling techniques. Journal of Coastal Research 6 (1), 111–120.
Stafford, D.B., 1971. An aerial photographic technique for beach erosion surveys in North Carolina. U.S. Army Corps of Engineers, Coastal Engineering Research Center, 115p. In: Moore, L.J., Ruggiero, P., List, J.H., 2006. Comparing mean high water and high water line shorelines: should proxy-datum offsets be incorporated into shoreline change analysis? Journal of Coastal Research 22(4), 894–905.
Stein, S., Okal, E.A., 2005. Speed and size of the Sumatra earthquake. Nature 434, 581–582.
Subarya, C., Chlieh, M., Prawirodirdjo, L., Avouac, J.-P., Bock, Y., Sieh, K., 2006. Plate-boundary deformation associated with the great Sumatra–Andaman earthquake. Nature 440, 46–51.
Umitsu, M., Tanavud, C., Patanakanog, B., 2007. Effects of landforms on tsunami flow in the plains of Banda Aceh, Indonesia, and Nam Khem, Thailand. Marine Geology 242, 141–153.
UP-PSDA, 2003. Report on oceanography measurements and wave analysis. Detail design of Syiah Kuala beach, Banda Aceh City, Flood and coastal safety project, Civil Work Department, Nanggroe Aceh Darussalam, Province, Banda Aceh. (In Indonesian).
Waltham, T., 2005. The Asian Tsunami disaster, December 2004. Geology Today 21 (1), 22–26.
Zhang, K., Whitman, D., Leatherman, S., Robertson, W., 2005. Quantification of beach changes caused by hurricane Floyd along Florida's coast using Airborne laser surveys. Journal of Coastal Research 21 (1), 123–134.